Nanoscale

Understanding Functional Group and Assembly Dynamics in Temperature Responsive Systems Leads to Design Principles for Enzyme Responsive Assemblies

Journal:	*Nanoscale*
Manuscript ID	NR-ART-03-2021-002000.R1
Article Type:	Paper
Date Submitted by the Author:	02-Jun-2021
Complete List of Authors:	Liu, Hongxu; University of Massachusetts Amherst Lionello, Chiara; Politecnico di Torino Westley, Jenna; University of Massachusetts Amherst Cardellini, Annalisa; Politecnico di Torino Huynh, Uyen; University of Massachusetts Amherst Pavan, Giovanni; Politecnico di Torino Thayumanavan, Sankaran; University of Massachusetts Amherst

ARTICLE

Understanding Functional Group and Assembly Dynamics in Temperature Responsive Systems Leads to Design Principles for Enzyme Responsive Assemblies

Received 00th January 20xx,
Accepted 00th January 20xx

DOI: 10.1039/x0xx00000x

Hongxu Liu,[a] Chiara Lionello,[b] Jenna Westley,[a] Annalisa Cardellini,[b] Uyen Huynh,[a] Giovanni M. Pavan,*[b,c] and S. Thayumanavan*[a]

Understanding the molecular rules behind the dynamics of supramolecular assemblies is fundamentally important for the rational design of responsive assemblies with tunable properties. Herein, we report that the dynamics of temperature-sensitive supramolecular assemblies is not only affected by the dehydration of oligoethylene glycol (OEG) motifs, but also by the thermally-promoted molecular motions. These counteracting features set up a dynamics transition point (DTP) that can be modulated with subtle variations in a small hydrophobic patch on the hydrophilic face of the amphiphilic assembly. Understanding the structural factors that control the dynamics of the assemblies leads to rational design of enzyme-responsive assemblies with tunable temperature responsive profiles.

Introduction

Stimuli-responsive nanoassemblies have drawn attention due to their potential applications in a variety of fields such as drug delivery, diagnosis, and bioseparation.[1–8] Among the large number of stimuli-responsive materials,[1,9–12] temperature sensitive polymeric assemblies have attracted particular attention in the context of its responsive phase change at the so-called lower critical solution temperature (LCST).[13–18] Oligo- and poly-ethylene glycol based polymers, along with poly(*N*-alkylacrylamides), have been especially studied, where the responsive characteristics arise from the breakage of the hydrogen bonding with water at higher temperatures.[19–23] The disrupted hydrogen bonding manifests as enhanced hydrophobicity of the polymer, leading to a phase change.[24,25] This temperature-induced phase change is often taken to be an abrupt change in hydrophobicity at a specific temperature, which could be viewed as a cooperative change in their hydrogen bonding features. Recently, however, it was observed that certain oligoethyleneglycol (OEG) based nanoassemblies exhibit a more subtle morphological transition at temperatures below LCST, a sub-LCST transition, where the sizes of the assemblies was found to vary substantially.[26] However, the factors entailing the sub-LCST behavior and the dynamics of these assemblies are not well understood. For example, not all OEG-based amphiphiles exhibit the sub-LCST behavior and the behavior may vary with OEG chain length.[27–29] In the quest of understanding the features that control temperature-dependent dynamics of amphiphilic assemblies, we were particularly interested in understanding the impact of introducing small hydrophobic patches on the solvent-exposed hydrophilic surface of the assemblies upon their temperature-dependent dynamics (Fig. 1). Also, note that temperature can alter dynamics in amphiphilic assemblies in two disparate ways. On one hand, the classical relationship between temperature and dynamics is that thermally-promoted molecular motion should make nanoassemblies more dynamic.[30–32] On the other hand, in the context of the sub-LCST behavior, we found that the thermal dehydration of the hydrophilic OEG groups can cause molecular assemblies to be more frozen at higher temperatures.[26] Here, temperature would have an inverse relationship with dynamics. We became interested in understanding the balance between these two factors in amphiphilic nanoassemblies.

To understand the aforementioned questions, we herein employ the fluorescent tools into nanoassemblies as the readout-signal. Fluorescent methods have been previously used to study inter- and intramolecular interactions and microviscosity change within assemblies.[33–36] However, only a few of them discussed the correlation of fluorescent signals with the structural and dynamical property change in molecular assemblies.[37–39] 7-diethylaminocoumarin is utilized as the dynamics probe, as this fluorophore has strong monomer and excimer emissions at distinct wavelengths.[40,41] We ascertain that thermally-induced change in dynamics and assembly evolution can thus be studied by incorporating this fluorophore

[a] Department of Chemistry, University of Massachusetts Amherst, Amherst, Massachusetts 01003, United States. Email: thai@chem.umass.edu
[b] Department of Applied Science and Technology, Politecnico di Torino, 10129 Torino, Italy. Email: giovanni.pavan@polito.it
[c] Department of Innovative Technologies, University of Applied Sciences and Arts of Southern Switzerland, CH-6962 Viganello, Switzerland.

Electronic Supplementary Information (ESI) available: [details of any supplementary information available should be included here]. See DOI: 10.1039/x0xx00000x

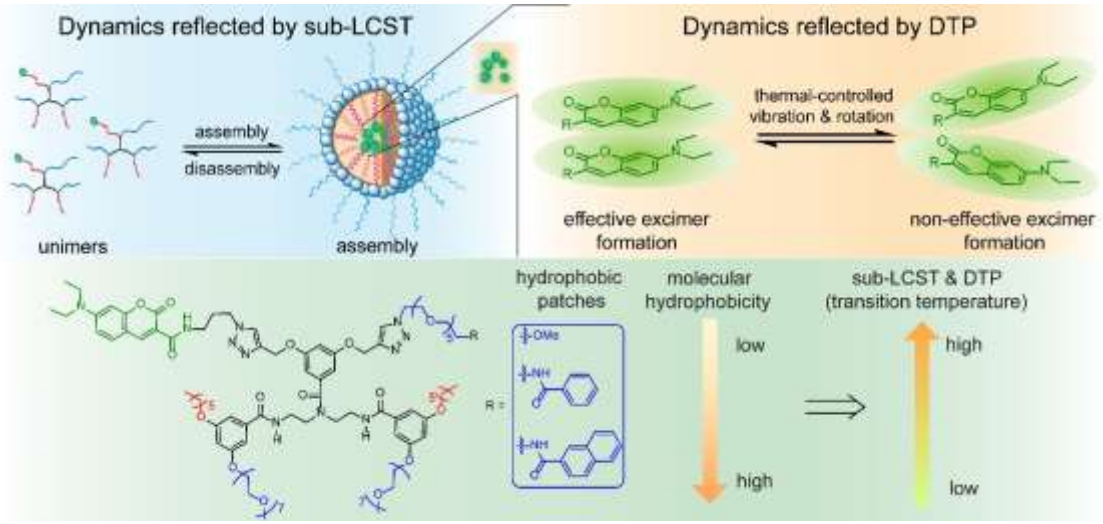

Fig 1. Schematic presentation of the assembly dynamics reflected by sub-LCST and DTP and their relationship with the molecular hydrophobicity.

in amphiphilic assemblies. Experimental results corroborating molecular modeling, provide a molecular level insight into temperature change effects on the structural dynamics of these complex self-assembled systems. Finally, we exemplify the implications of this fundamental understanding with a predictive molecular design of an enzyme-responsive assembly that transitions from a less dynamic to a more dynamic assembly at ambient temperature.

Results and discussion

Molecular Structure and Synthesis. To test whether 7-diethylaminocoumarin-modified amphiphilic oligomers lend themselves for this study, we first designed and synthesized an amphiphilic oligomer, **EG7-C6-Ph**, shown in Fig. 2. The amphiphilic scaffolds can be precisely functionalized in their hydrophobic and hydrophilic faces, allowing a fine modulation of the amphiphilicity. Briefly, the backbone of the amphiphilic molecules is based on diethylenetriamine, where the terminal amino moieties are substituted with amphiphilic benzamides. The hydrophilic part of the molecule is based on a hexyl chain (C6). The central amine is also functionalized with an amphiphilic benzamide, where the hydrophobic side of the molecule contains the 7-diethylaminocoumarin fluorophore moiety. The hydrophilic side of this benzamide contains a hexaethyleneglycol moiety that is terminated with a phenyl group (Ph). It is the location of the phenyl group that becomes the point of modification for us to introduce the small hydrophobic patches in the oligoethyleneglycol-based hydrophilic surface. This molecule was synthesized by first selectively introducing the amphiphilic blocks to diethylenetriamine core, then labeling with the coumarin moiety through click chemistry (see SI for synthetic details).

Preparation and Characterization of Assemblies. With the molecule in hand, we studied the formation of nanoassemblies in aqueous solution and their thermal-responsive behaviors. The assembly was prepared by first dissolving **EG7-C6-Ph** in acetone, followed by adding it dropwise into deionized water (see SI for details). After evaporating the organic solvent, the solution was diluted to 25 µM and the size of assembly was found to be ~65 nm as characterized using dynamic light scattering (DLS). The critical aggregation concentration (CAC) was evaluated using the previously developed dye encapsulation method and was found to be 21 µM (Fig. S1).[41,42]

Temperature-dependent Fluorescence Change of EG7-C6-Ph. We then studied the temperature-dependent variations in the

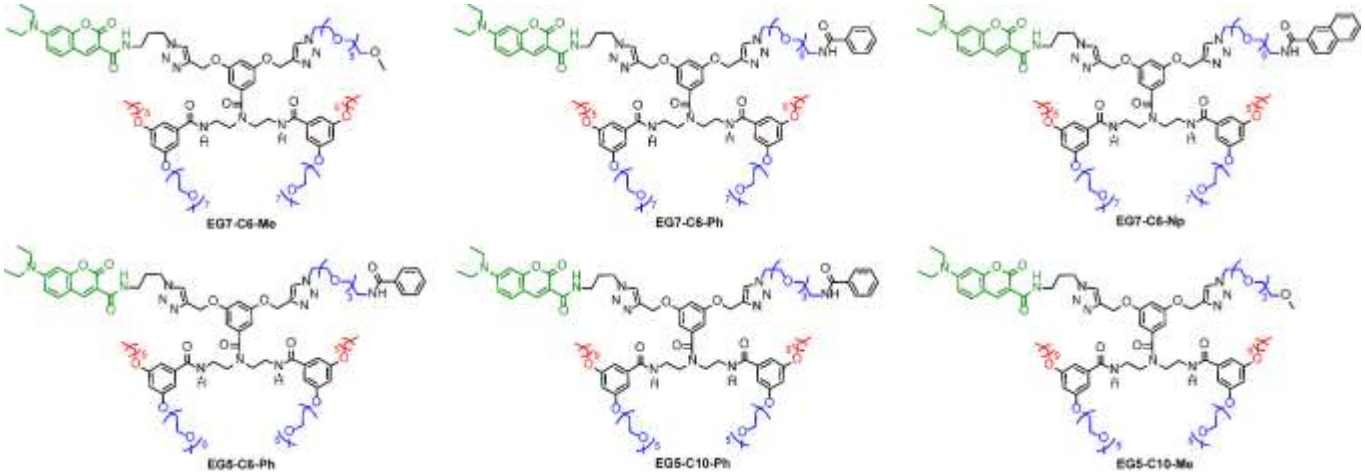

Fig 2. Structures of amphiphilic oligomers investigated in this study.

fluorescence behavior of the assemblies. The assemblies exhibit two fluorescence emission peaks with maxima at 479 nm and 536 nm, corresponding to the monomer and excimer fluorescence of the aminocoumarin respectively (Fig. 3a). When increasing temperature, the total fluorescence intensity of both peaks decreased, likely due to increased non-radiative decay at higher temperatures.[43] Interestingly, the ratio of the monomer (I_M) to excimer emission intensity (I_E) has two distinct temperature-dependent trends. In particular, the I_M/I_E ratio gradually decreases from 5 to 30 °C, then increases from 30 to 65 °C (Fig. 3b). Note that the excimer emission is indicative of two fluorophore moieties in the nanoassembly in close proximity within the nanoassembly. Therefore, a decrease in I_M/I_E ratio is taken to suggest a tighter assembly. Between 5 and 30 °C, when increasing temperature, the molecules approach to a more hydrophobic-like behavior due to the disruption of hydrogen-bonding between OEG moieties and water. Then the enhanced hydrophobic interaction leads to more compact assemblies, resulting in higher possibility for excimer formation. However, increasing temperature between 30 and 65 °C enhances the thermally-promoted molecular motions, making the assemblies more dynamic and leading to lesser excimer formation. As a consequence, the I_M/I_E ratio gradually increases.

Coarse-Grained MD Simulations of the Temperature-responsive Assemblies of EG7-C6-Ph. To further test our hypothesis and understand the correlation between fluorescent signals and molecular structural properties in response to temperature changes, we developed all atom (AA) and coarse-grained (CG) models for the assemblies. In particular, the CG models for the molecules, built based on the MARINI force field, have been optimized for the best agreement with the AA models using the recently developed Swarm-CG software[44]. Molecular dynamics (MD) simulations were carried out for a single assembly respectively at 10 °C, 30 °C and 60 °C GROMACS 2018.6[45]. Fig. 3d shows a snapshot of the AA and CG monomer models and the structure of a 50 dendrons assembly (EG7-C6-Ph) from the MD simulations in water (see SI for details). The radius of gyration, R, of the assemblies and their sub-groups, estimated from the CG-MD simulations, is selected as the indicator to study how the assembly structure and compactness change with temperatures (Fig. S4). From the CG-MD simulations of the assemblies, we calculated the R values of the hexyl (R_{hexyl}), coumarin (R_{Coum}) and PEG (R_{PEG}) groups in the assemblies, as well as the global gyration radius of the various assemblies (R_a). As is shown in Fig. 3e, the ratio between the R of the various groups and the R_a of the assemblies provide information on the composition of the structure of the assemblies. R/R_a >1 indicate that the groups are exposed on the surface of the assembly (and to the solvent), while R/R_a becomes <1 for groups buried in the assembly interior. Monitoring the R/R_a as function of temperature allows to observe structural rearrangements following to temperature changes. Both ratios R_{hexyl}/R_a and R_{Coum}/R_a, being lower than 1, reveal their hydrophobic nature avoiding water contacts and placing into the inner region of the assembly. On the other hand, the hydrophilic PEG chains present R_{PEG}/R_a >1, thus they arrange in the most external region of the assembly, remarking their affinity with water. Moreover, as shown in Fig. 3f, the gyration radius of assembly, R_a, at 30 °C is lower than those at both 10 °C and 60 °C. These results have the same trend as our fluorescence results in Fig. 3b and confirms the comprehensive effect of PEG dehydration and thermally-promoted molecular motion hypotheses. In fact, because of temperature breaking hydrogen bonds, a more hydrophobic and compact assembly,

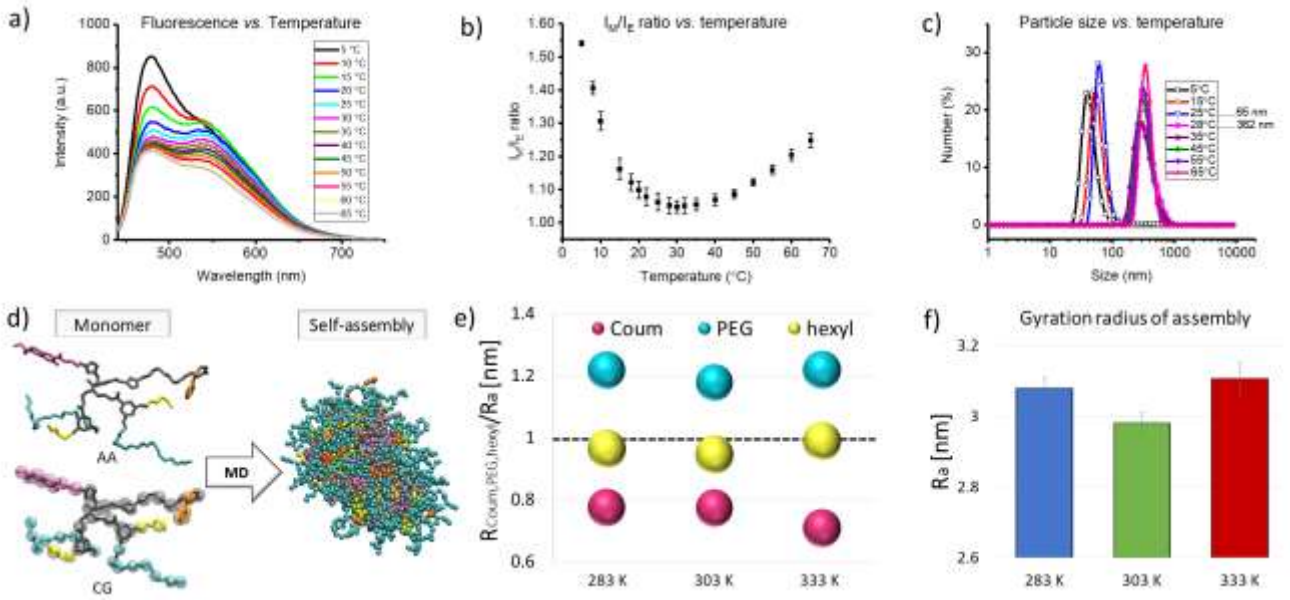

Fig 3. Characterization of **EG7-C6-Ph**-constituted assemblies (25 μM): (a) Fluorescence of the assemblies at different temperature. (b) I_M/I_E ratio versus temperature. (c) Particle sizes at different temperature. (d) All-Atom (AA) and Coarse-Grain (CG) Molecular Dynamics (MD) model **of EG7-C6-Ph**. (e) Ratio between the gyration radius, R, of the hexyl, Coumarin, PEG groups in the dendrons and the R of the entire assembly (Ra). R values greater than 1 indicates groups exposed on the surface of the assembly, while R smaller than 1 is indicative of groups buried in the assembly interior. (f) Gyration radius of the **EG7-C6-Ph** assemblies at 283 K, 303 K, and 333 K.

with lower radius of gyration is expected at 30 °C; after that, because of the accelerated molecular motion, the gyration radius of assembly increases. Moreover, the higher PEG-water interaction at 10 °C demonstrates that PEG units are more hydrophilic at lower temperature (Fig. S5b). On the other hand, lower PEG-PEG contact (Fig. S5a) and higher hydrophobic-water contact numbers at 60 °C (Fig. S5c) suggest the swelling of assemblies. It is worth noting that the thermal-enhanced motion of the amphiphiles, occurring while increasing the temperature from 30 °C to 60 °C, causes an increased probability for water penetration inside the soft core of the NP. The hydrophobic coumarin groups become thus more in contact with water (see also Fig. S5e). As a result, at T = 60 °C, the coumarin CG particles, tend to collapse in a more compact way because of their hydrophobic nature, as demonstrated by the reduction of R_{Coum}/R_a parameter in Fig. 3e.

Sub-LCST Behavior of EG7-C6-Ph. To further explore if the observed decrease in the I_M/I_E ratio at the lower temperature range can indeed be attributed to the sub-LCST phenomenon, we tested the evolution of assembly size with temperature. Dynamic light scattering (DLS) experiments show that the assembly size does sharply increase from 65 nm to 362 nm at about 28 °C, which is akin to the sub-LCST behavior (Fig. 3c).[27] This size transition temperature is close to 30 °C, i.e. the temperature corresponding to the minimum in the I_M/I_E ratio profile (Fig. 3b). We surmised that the trend observed at lower temperatures is indeed a sub-LCST like behavior. Previously the size change and the associated change in assembly dynamics was thought about as a sharp change in the hydration of the OEG moieties. The slow decrease in the I_M/I_E ratio with temperature in the current experiments suggest that the dehydration of OEG moieties continuously changes with temperature, but after the sub-LCST transition any further change due to dehydration is negligible.

Correlations of Molecular Structures with DTPs and sub-LCSTs. We then became interested in the idea of altering the hydrophobic functionality on the hydrophilic surface and investigating its influence on the temperature sensitivity.

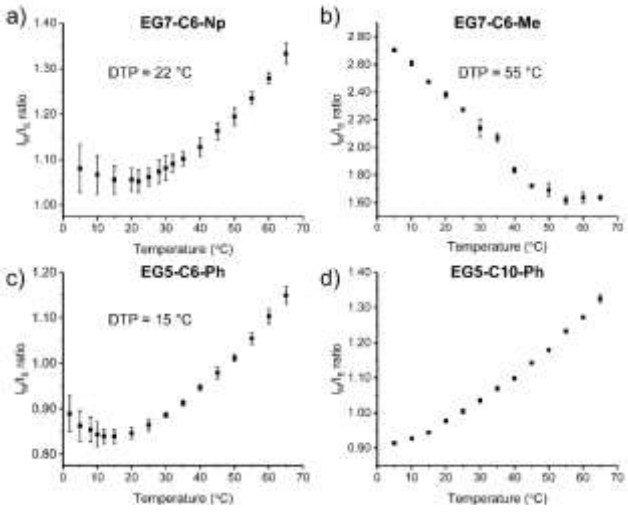

Fig 4. Correlation between I_M/I_E ratio and temperature of amphiphile (25 μM): (a) **EG7-C6-Np**, (b) **EG7-C6-Me**, (c) **EG5-C6-Ph**, (d) **EG5-C10-Ph**.

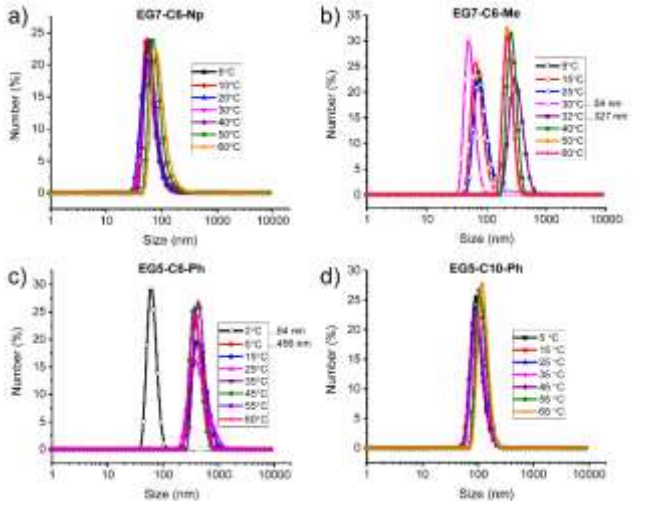

Fig 5. Correlation between particle sizes and temperature of amphiphile (25 μM): (a) **EG7-C6-Np**, (b) **EG7-C6-Me**, (c) **EG5-C6-Ph**, (d) **EG5-C10-Ph**.

Accordingly, we synthesized **EG7-C6-Me** and **EG7-C6-Np**, where the phenyl (Ph) group at the hydrophilic terminus of the central amine are changed to methyl (Me) and naphthyl (Np) groups respectively (Fig. 2). We chose these two functionalities, because when analyzed with MD simulations, the comparison of the gyration radius of Me and Np residues with the entire assembly has reported R_{Me}/R_a = 1.1 and R_{Np}/R_a = 0.76 respectively, thereby exhibiting a more hydrophilic and hydrophobic character than the phenyl, respectively (Fig. S6). These further oligomer case studies allow us to correlate the sub-LCSTs and DTPs to the chemical design of assembly sub-units.

We were particularly interested in the minimum of the I_M/I_E plot, which can be taken as the 'dynamics transition point' (DTP). Because it is at this point that the dynamics of the functional groups embedded in these assemblies transition from being controlled by the sub-LCST behavior (dehydration of OEG) to thermally-controlled molecular motions. In the case of **EG7-C6-Np**, the DTP is 22 °C (Fig. 4a). Interestingly, no sharp size transition is observed for this assembly (Fig. 5a). On the other hand, in **EG7-C6-Me**, the DTP appears at 55 °C (Fig. 4b) with a size transition temperature at 32 °C (Fig. 5b). These results show that variations of a small terminal hydrophobic moiety in just one of the hydrophilic chains can lead to substantial change in both the DTP and particle size transition (sub-LCST) temperatures, although they are not identically affected. While it is understandable that OEG dehydration requires higher temperature when there is an increase in hydrophilicity of the functional group, it is interesting that a single functional group change was able to cause a rather significant change.

Note that although DTP temperature and the sub-LCST are close to each other in **EG7-C6-Ph**, DTP was found to be higher than the sub-LCST for the other two molecules, **EG7-C6-Me** and **EG7-C6-Np**. This is understandable, because although both these phenomena are related to temperature-induced dehydration of the hydrophilic functionalities, it is important to recognize that these two temperatures indicate very different characteristics of the assembly. DTP is a measure of the impact of change in

hydration and the thermal-promoted molecular motions on the overall dynamics of a fluorophore embedded in the assembly. The sub-LCST on the other hand is a distinct change in the assembly size, presumably because of the change in the overall hydrophilic-lipophilic balance in the molecule. It has been previously shown however that the well-hydrated smaller assemblies at lower temperatures are more dynamic, compared to the large assemblies at higher temperatures.[26]

What then is the exact difference in the information gleaned from the DTP-based change in dynamics and sub-LCST based change in dynamics? The difference is the length scale of the processes. DTP-based dynamics provides insights into the effect of temperature on functional groups that are embedded in the hydrophobic interiors of an assembly, while the sub-LCST dynamics focuses on the entire host molecule with respect to unimer-aggregate equilibrium (Fig. 1). Below sub-LCST, the dynamics of the equilibrium between the unimeric and the aggregated state of the assembly is fast.[26] Above sub-LCST, such self-assembly dynamics tends to slow down, preventing remarkable change in the assembly state configuration and limiting the unimeric exchange. At a functional group scale, the dynamics of the fluorogenic functionality would change commensurately with the unimer below the sub-LCST. The fact that DTP temperature is higher than sub-LCST, however, suggests that the dynamics of the fluorogenic functionality is continuing to evolve with temperature above the sub-LCST. This evolution is dominated by the temperature-induced dehydration of the OEG functionalities in the assembly below the DTP temperature, while it is dominated by thermal motions when above that temperature. Perhaps, the most important take-home from this finding is that the sub-LCST does not necessarily represent a sharp change in the dehydration of the OEG moieties and that the functional group dynamics is modulated by temperature even beyond the sub-LCST.

We then became interested in investigating if (*i*) the DTP temperature is consistently higher than the sub-LCST; (*ii*) hydrophobicity variations in both hydrophilic and hydrophobic faces of the amphiphile can generally dictate the DTP and sub-LCST trends. Accordingly, we first synthesized **EG5-C6-Ph**, which is only different from **EG7-C6-Ph** with a shorter OEG length. As the overall hydrophobicity of **EG5-C6-Ph** is higher, DTP temperature and sub-LCST temperature are both expected to be lower than that of **EG7-C6-Ph**. Indeed, the DTP temperature of the former molecule shifts to 15 °C, compared to 30 °C for the latter (Fig. 4c and 3b). The sub-LCST of **EG5-C6-Ph** and **EG7-C6-Ph** were found to be ~5 °C and ~28 °C

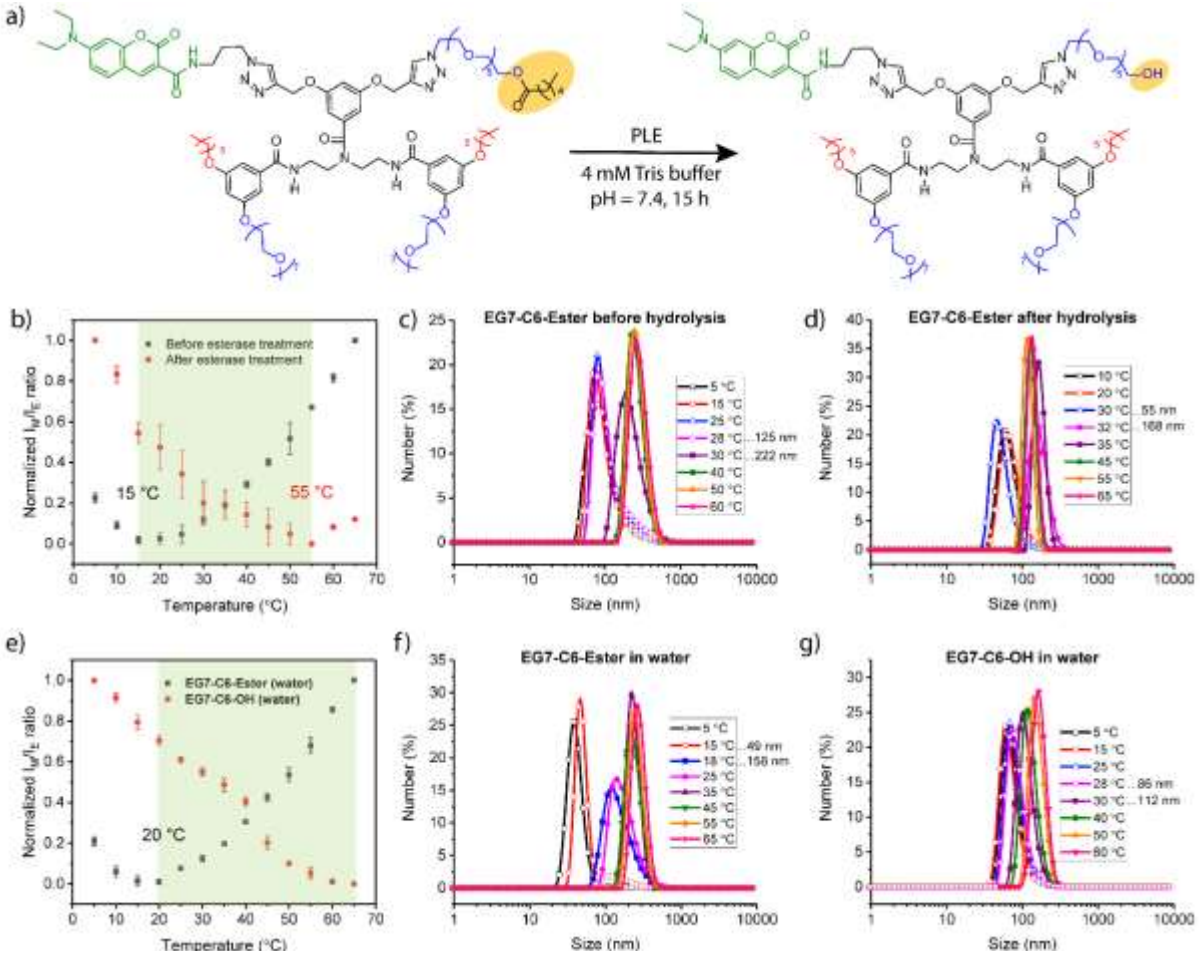

Fig 6. (a) Molecular structure transformation before and after PLE treatment. (b) Comparison of normalized I_M/I_E ratio versus temperature before and after PLE treatment. In the green shadow region, the dynamics of **EG7-C6-Ester** and the product after enzymatic treatment have inverse trends while increasing temperature: **EG7-C6-Ester** increases but the product decreases. Correlation between particle sizes and temperature of **EG7-C6-Ester** before (c) and after (d) esterase treatment. (e) Comparison of normalized I_M/I_E ratio versus temperature for **EG7-C6-Ester** and **EG7-C6-OH** in water. Correlation between particle sizes and temperature for **EG7-C6-Ester** (f) and **EG7-C6-OH** (g) in water.

respectively (Fig. 5c and 3c). Similarly, **EG5-C10-Ph** has increased hydrophobicity, compared to **EG5-C6-Ph**, due to increase in the hydrophobic chain length to decyl from hexyl unit. In this case, the DTP temperature and sub-LCST for **EG5-C10-Ph** were not detectible (Fig. 4d and 5d). The positive slope in I_M/I_E ratio vs. temperature suggests that these two transitions points are presumably below 0 °C. Considering that this molecule is more hydrophobic than **EG5-C6-Ph**, which already exhibits low transition temperatures, such results are understandable. Because this transition is not observable, we used the **EG5-C10** scaffold, but made a single point mutation from phenyl to methyl moiety at the central amphiphilic unit to generate **EG5-C10-Me** (Fig. 2). The DTP temperature and sub-LCST now were found to be at 25 and 15 °C, respectively (Fig. S3a and S3b). Overall, all these systematic structural variations showed that hydrophobicity can significantly influence these transitions, even when there is a single change in the amphiphile. Moreover, the DTP temperature was found to be always lower than the sub-LCST. These observations are thus consistent with our hypotheses.

Enzyme-triggered Temperature-responsive Behavior Change. Finally, we resorted to demonstrating the utility of these findings in developing responsive assemblies that straddles beyond temperature sensitivity. We hypothesized that our finding that single change in the hydrophobicity of a functional group on the solvent-exposed face of the hydrophilic unit can have a significant impact on assembly properties, lending itself to designing systems that can be transitioned from a static system to a dynamic system for any stimulus. We were particularly interested in executing the stimulus-induced change in the hydrophilic face, because this functionality would be more accessible. Nowhere is this accessibility more important than in enzyme-responsive systems.[41,46,47] Therefore, as a proof-of-principle, we designed an esterase enzyme responsive system by embedding one hexyl-ester moiety on the hydrophilic face of the central amine in the amphiphile. Structure of the molecule **EG7-C6-Ester** is shown Fig. 6a. Upon treatment with porcine liver esterase (PLE), this hexyl ester moiety gets converted to the corresponding alcohol **EG7-C6-OH**. Because of this conversion, the DTP temperature shifted from 15 °C to 55 °C (Fig. 6b). This means, before PLE treatment, the assembly is becoming more dynamic when varying temperature from 15 °C to 55 °C, while by contrast being less dynamic after the treatment. Accordingly, the sub-LCST of changed slightly from 30 °C to 32 °C (Fig. 6c and 6d), although it is not as distinct as expected likely because of the impact of the Tris base. When the assembly of **EG7-C6-Ester** and **EG7-C6-OH** were tested in water, the DTPs were found to be 20 °C and no less than 65 °C (above the experiment limit) respectively (Fig. 6e), which are in line with the results obtained before and after PLE treatment in Tris buffer. The corresponding sub-LCSTs are 18 °C and 30 °C (Fig. 6f and 6g). These results also demonstrate that Tris base indeed affects absolute values of both the DTPs and sub-LCSTs, but the relative trends are not affected. Overall, the outcomes of our study led to rational design of an amphiphile that exhibits substantial changes in the dynamics of the embedded functional groups and the unimer-aggregate equilibrium in response to an enzymatic stimulus at ambient temperature.

Conclusions

In summary, we have investigated the dynamics of individual functional groups and the entire molecule in temperature responsive assemblies through judicial variations in the structures of oligomeric amphiphiles. We show here that: (i) there exists a dynamics transition point (DTP), where the temperature dependent alteration in the dynamics of the functional group switches from dependence on the dehydration of OEG moieties to thermally-promoted molecular motions; (ii) variations in the hydrophobicity of the amphiphilic units, including a single functional group change in the hydrophilic face of the molecule, substantially impact DTP temperature and sub-LCST related size transitions in these nanoassemblies; (iii) although the trends in DTP and sub-LCST are similar, the former temperature is consistently higher than the latter. This observation is rationalized based on the length scale of functional group dynamics vs. molecular assembly dynamics; (iv) the effect of single point mutations in structures has the potential to be translated broadly to other stimuli, which was demonstrated with a rational design of an enzyme responsive assembly. Overall, the fundamental findings in this manuscript have implications in designing responsive supramolecular assemblies, well beyond realms of temperature sensitive systems.

Author Contributions

H. L., G. M. P. and S. T. conceived the idea and designed the experiments and the simulations. H. L. conducted the experiments with the help of J. W. and U. H. for some of the fluorescence test. C. L. and A. C. performed simulations. H. L., C. L., A. C., G. M. P. and S. T. analyzed the data and wrote the manuscript. All authors reviewed the manuscript.

Conflicts of interest

The authors declare no competing financial interest.

Acknowledgements

We thank U.S. Army Research Office (W911NF-15-1-0568 and W911NF1810355) for supporting this work. G.M.P. also acknowledges the funding received by the Swiss National Science Foundation (SNSF grant 200021_175735) and by the European Research Council (ERC) under the European Union's Horizon 2020 research and innovation program (grant agreement no. 818776 – DYNAPOL). The authors also acknowledge the computational resources provided by the Swiss National Supercomputing Center (CSCS) and by CINECA.

Notes and references

1 H. Shigemitsu and I. Hamachi, *Acc. Chem. Res.*, 2017, **50**, 740–750.
2 G. Liu, G. Zhang, J. Hu, X. Wang, M. Zhu and S. Liu, *J. Am. Chem. Soc.*, 2015, **137**, 11645–11655.
3 X. Liu, K. Jia, Y. Wang, W. Shao, C. Yao, L. Peng, D. Zhang, X. Y. Hu and L. Wang, *ACS Appl. Mater. Interfaces*, 2017, **9**, 4843–4850.
4 E. G. Kelley, J. N. L. Albert, M. O. Sullivan and T. H. Epps, *Chem. Soc. Rev.*, 2013, **42**, 7057–7071.
5 M. Elsabahy, G. S. Heo, S. Lim, G. Sun and K. L. Wooley, *Chem. Rev.*, 2015, **115**, 10967–11011.
6 A. P. Blum, J. K. Kammeyer, A. M. Rush, C. E. Callmann, M. E. Hahn and N. C. Gianneschi, *J. Am. Chem. Soc.*, 2015, **137**, 2140–2154.
7 D. Astruc, E. Boisselier and C. Ornelas, *Chem. Rev.*, 2010, **110**, 1857–1959.
8 S. H. Medina and M. E. H. El-Sayed, *Chem. Rev.*, 2009, **109**, 3141–3157.
9 X. Yan, F. Wang, B. Zheng and F. Huang, *Chem. Soc. Rev.*, 2012, **41**, 6042–6065.
10 K. R. Raghupathi, J. Guo, O. Munkhbat, P. Rangadurai and S. Thayumanavan, *Acc. Chem. Res.*, 2014, **47**, 2200–2211.
11 M. E. Roth, O. Green, S. Gnaim and D. Shabat, *Chem. Rev.*, 2016, **116**, 1309–1352.
12 H. Yang, B. Yuan, X. Zhang and O. A. Scherman, *Acc. Chem. Res.*, 2014, **47**, 2106–2115.
13 B. J. Rancatore, C. E. Mauldin, J. M. J. Fréchet and T. Xu, *Macromolecules*, 2012, **45**, 8292–8299.
14 Y. Z. You, K. K. Kalebaila, S. L. Brock and D. Oupický, *Chem. Mater.*, 2008, **20**, 3354–3359.
15 H. Wei, X. Z. Zhang, H. Cheng, W. Q. Chen, S. X. Cheng and R. X. Zhuo, *J. Control. Release*, 2006, **116**, 266–274.
16 P. Pan, M. Fujita, W. Y. Ooi, K. Sudesh, T. Takarada, A. Goto and M. Maeda, *Langmuir*, 2012, **28**, 14347–14356.
17 M. Karimi, P. Sahandi Zangabad, A. Ghasemi, M. Amiri, M. Bahrami, H. Malekzad, H. Ghahramanzadeh Asl, Z. Mahdieh, M. Bozorgomid, A. Ghasemi, M. R. Rahmani Taji Boyuk and M. R. Hamblin, *ACS Appl. Mater. Interfaces*, 2016, **8**, 21107–21133.
18 V. Albright, A. Palanisamy, Q. Zhou, V. Selin and S. A. Sukhishvili, *Langmuir*, 2018, **35**, 10677–10688.
19 Z. Al-Ahmady and K. Kostarelos, *Chem. Rev.*, 2016, **116**, 3883–3918.
20 J. Dey, R. Ghosh and R. Das Mahapatra, *Langmuir*, 2019, **35**, 848–861.
21 M. M. Ali and H. D. H. Stöver, *Macromolecules*, 2004, **37**, 5219–5227.
22 L. Hou and P. Wu, *Macromolecules*, 2016, **49**, 6095–6100.
23 K. Zheng, J. Ren and J. He, *Macromolecules*, , DOI:10.1021/acs.macromol.9b00920.
24 D. Roy, W. L. A. Brooks and B. S. Sumerlin, *Chem. Soc. Rev.*, 2013, **42**, 7214–7243.
25 K. Kumbhakar, B. Saha, P. De and R. Biswas, *J. Phys. Chem. B*, 2019, **123**, 11042–11054.
26 J. M. Fuller, K. R. Raghupathi, R. R. Ramireddy, A. V. Subrahmanyam, V. Yesilyurt and S. Thayumanavan, *J. Am. Chem. Soc.*, 2013, **135**, 8947–8954.
27 K. R. Raghupathi, U. Sridhar, K. Byrne, K. Raghupathi and S. Thayumanavan, *J. Am. Chem. Soc.*, 2015, **137**, 5308–5311.
28 G. M. Pavan, A. Barducci, L. Albertazzi and M. Parrinello, *Soft Matter*, 2013, **9**, 2593–2597.
29 O. Munkhbat, M. Garzoni, K. R. Raghupathi, G. M. Pavan and S. Thayumanavan, *Langmuir*, 2016, **32**, 2874–2881.
30 D. W. Fu, W. Zhang, H. L. Cai, Y. Zhang, J. Z. Ge, R. G. Xiong and S. D. Huang, *J. Am. Chem. Soc.*, 2011, **133**, 12780–12786.
31 J. Liu and J. C. Conboy, *J. Am. Chem. Soc.*, 2004, **126**, 8376–8377.
32 P. Alam, N. L. C. Leung, Y. Cheng, H. Zhang, J. Liu, W. Wu, R. T. K. Kwok, J. W. Y. Lam, H. H. Y. Sung, I. D. Williams and B. Z. Tang, *Angew. Chemie - Int. Ed.*, 2019, **58**, 4536–4540.
33 L. Zhang, Q. Yin, J. Su and Q. Wu, *Macromolecules*, 2011, **44**, 6885–6890.
34 K. Nakashima, T. Anzai and Y. Fujimoto, *Langmuir*, 1994, **10**, 658–661.
35 M. Aoudia and M. A. J. Rodgers, *Langmuir*, 2006, **22**, 9175–9180.
36 Y. Shiraishi, T. Inoue and T. Hirai, *Langmuir*, 2010, **26**, 17505–17512.
37 T. Costa, M. D. G. Miguel, B. Lindman, K. Schillén and J. S. S. De Melo, *J. Phys. Chem. B*, 2005, **109**, 11478–11492.
38 J. Seixas De Melo, T. Costa, A. Francisco, A. L. Maçanita, S. Gago and I. S. Gonçalves, *Phys. Chem. Chem. Phys.*, 2007, **9**, 1370–1385.
39 L. Albertazzi, F. J. Martinez-Veracoechea, C. M. A. Leenders, I. K. Voets, D. Frenkel and E. W. Meijer, *Proc. Natl. Acad. Sci. U. S. A.*, 2013, **110**, 12203–12208.
40 I. Rosenbaum, A. J. Harnoy, E. Tirosh, M. Buzhor, M. Segal, L. Frid, R. Shaharabani, R. Avinery, R. Beck and R. J. Amir, *J. Am. Chem. Soc.*, 2015, **137**, 2276–2284.
41 N. Feiner-Gracia, M. Buzhor, E. Fuentes, S. Pujals, R. J. Amir and L. Albertazzi, *J. Am. Chem. Soc.*, 2017, **139**, 16677–16687.
42 Z. Jiang, H. Liu, H. He, A. E. Ribbe and S. Thayumanavan, *Macromolecules*, 2020, **53**, 2713–2723.
43 M. Aoudia, M. A. J. Rodgers and W. H. Wade, *J. Phys. Chem.*, 2005, **88**, 5008–5012.
44 C. Empereur-Mot, L. Pesce, G. Doni, D. Bochicchio, R. Capelli, C. Perego and G. M. Pavan, *ACS Omega*, 2020, **5**, 32823–32843.
45 M. J. Abraham, T. Murtola, R. Schulz, S. Páll, J. C. Smith, B. Hess and E. Lindah, *SoftwareX*, 2015, **1–2**, 19–25.
46 J. Guo, J. Zhuang, F. Wang, K. R. Raghupathi and S. Thayumanavan, *J. Am. Chem. Soc.*, 2014, **136**, 2220–2223.
47 J. Gao, H. Wang, J. Zhuang and S. Thayumanavan, *Chem. Sci.*, 2019, **10**, 3018–3024.